

Automatic Identification of Movement Variability

Miguel Xochicale

October 11, 2016

Mexican Tournament of Robotics 2013



Figure 1: Human-Robot Interaction Dance Demo

Research Questions

- Can we automatically identify the variability of:
 - (a) simple human activities (gestures) and
 - (b) complex human activities (dance)?
- Can we use the identification of variability as a index of skilled performance?

Activity Recognition Chain for Inertial Sensors

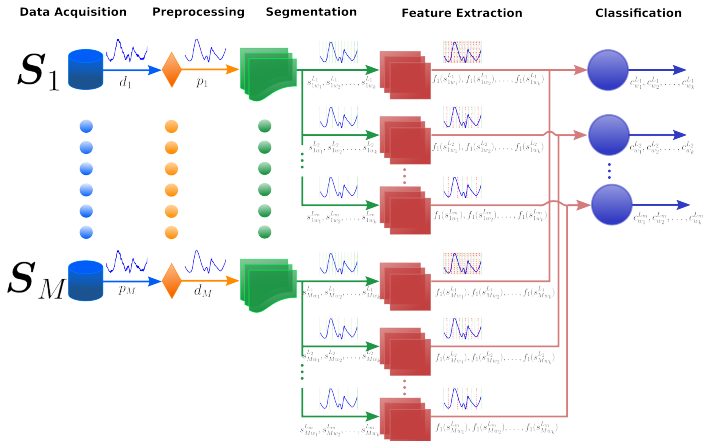


Figure 2: Window Size impact in ARC [Banos et al., 2014] .

Activity Recognition Chain from wearable sensors

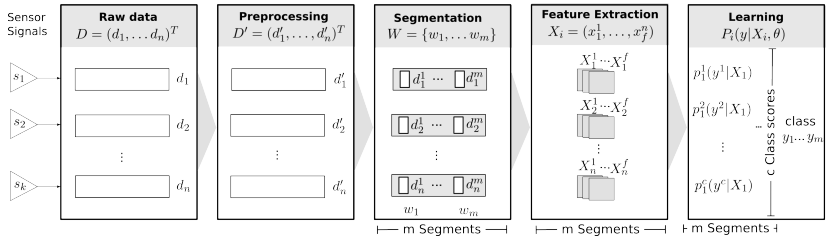


Figure 3: ARC to recognise activities from wearable sensors.
[Bulling et al., 2014].

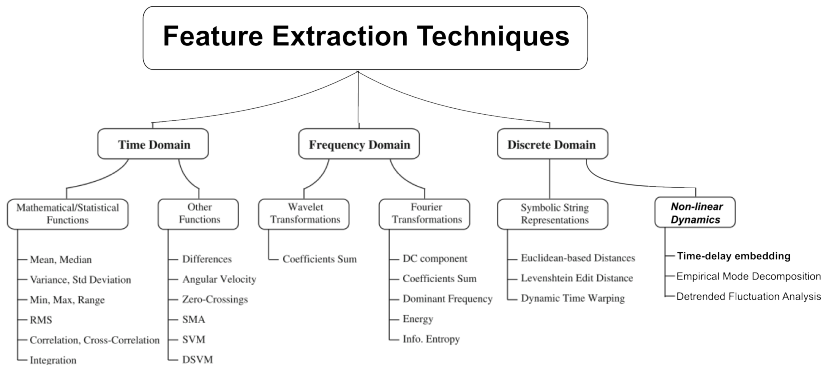


Figure 4: Techniques applied to accelerometer sensor signals for feature extraction

[**Figo et al., 2010, Liao et al., 2015, Gupta and Dallas, 2014, Fish and Khan, 2012, Zhang and Sawchuk, 2011**].

Time-delay embedding

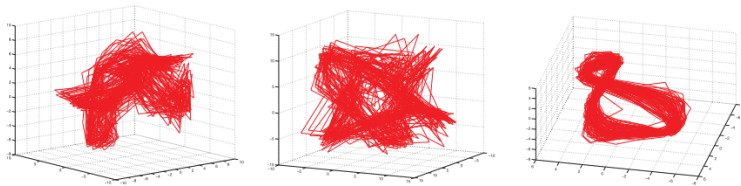


Figure 5: Time-delay embedding for walking (left), running (middle), and cycling (right) $m = 3$, $\tau = 4$.

[Frank et al., 2010, Frank et al., 2012].

Time-delay embedding

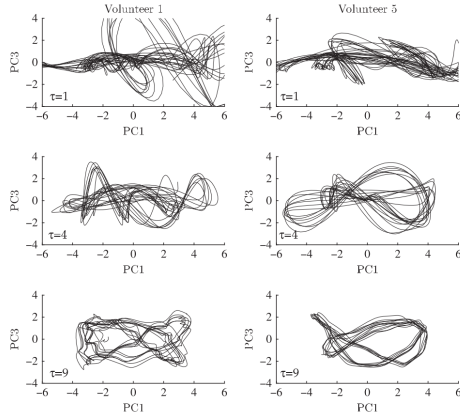


Figure 6: Time delay embeddings for gait patterns of two persons ($m = 20$ for $\tau = 1$, $\tau = 4$ and $\tau = 9$, respectively).
[Samà et al., 2013].

Intrinsic Structure Signal

Additive noise is created to introduce variance in the amplitude.

$$S_i = S_i^3 + \mathcal{N}(0, \sigma_a^2), \quad i = 1, 2, 3. \quad (1)$$

Where S is a regular sinusoid signal **[Hammerla et al., 2011]**.

*Low levels of additive noise correspond to precise movements.

Intrinsic Structure Signal

Structural noise is created to introduce variance in frequency , amplitude and local biases.

Algorithm 2 Add structural noise to a signal S .

Input: time-series $S = s_1 \dots s_L$, $s_i \in \mathbb{R}^3$, variance σ_s^2 .
Window length w_s

Output: Structurally distorted signal S^s .

```
1: for  $i = 1$  to  $3$  do
2:   for  $j = 1$  to  $L$ ,  $j = j + w_s$  do
3:      $v' \leftarrow \mathcal{N}(0, \sigma_s^2)$ 
4:      $S' = \text{sinusoid with frequency } |v'| \text{ of length } w_s$ 
5:      $S_{i,j \rightarrow j+w_s}^s = S_{i,j \rightarrow j+w_s} + S' \times \sigma_s^2$ 
6:   end for
7:    $S_{i,:}^s = \text{whiten}(S_{i,:})$ 
8: end for
9: return  $S^s$ 
```

Figure 7: Structural Noise Algorithm [Hammerla et al., 2011] .

Where S has a base frequency v_0 , and S^s is the distorted signal.

*Low levels of structural noise correspond to a well chosen strategy.

Structural Noise

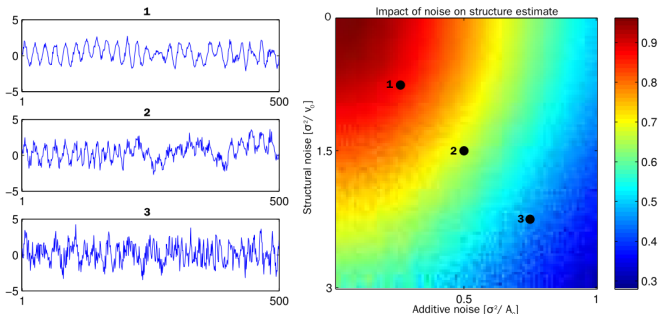


Figure 8: Three artificial signals that show the impact of additive noise and structural noise on sinusoid signals [Hammerla et al., 2011].

Additive noise – precision of movements
Structural noise – strategy for motion

Additive Noise and Structural Noise

Artificial signals are modeled using:

$$S(n) = A \sin(2\pi f_o n T_s) + \mathbf{N}n \quad (2)$$

where \mathbf{A} , \mathbf{F} and \mathbf{N} are normalised random vectors, n is the sample number and T_s is the sampling period.

A normalised random vector $\mathbf{X} = [\mathbf{X}_1, \mathbf{X}_2, \dots, \mathbf{X}_n]$ is expressed as $\mathbf{X} \sim \mathcal{N}(\mu_X, \sigma_X^2)$ with mean μ_X and variance σ_X^2

Additive Noise and Structural Noise

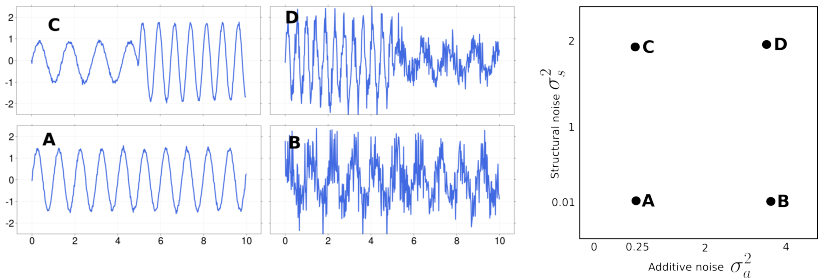


Figure 9: A, B, C and D plots present the variability of additive noise (σ_a^2) and structural noise (σ_s^2) on sinusoid signals with window lenght $w_s = 500$ [Hammerla 2011].

Variation per cycle

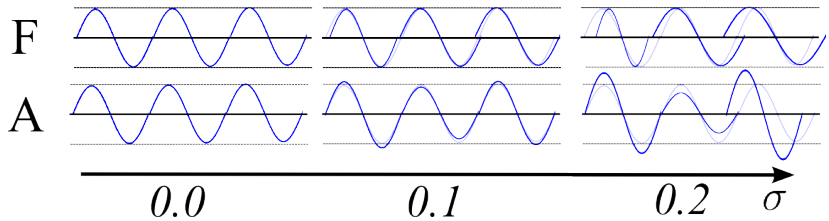


Figure 10: Variation of the Standard deviation for frequency and amplitude values per cycle

Gestures



Figure 11: Vertical, horizontal, diagonal, circular and wave-like
[Plötz et al., 2012] .

plotacc imu0 24022016-124306.csv

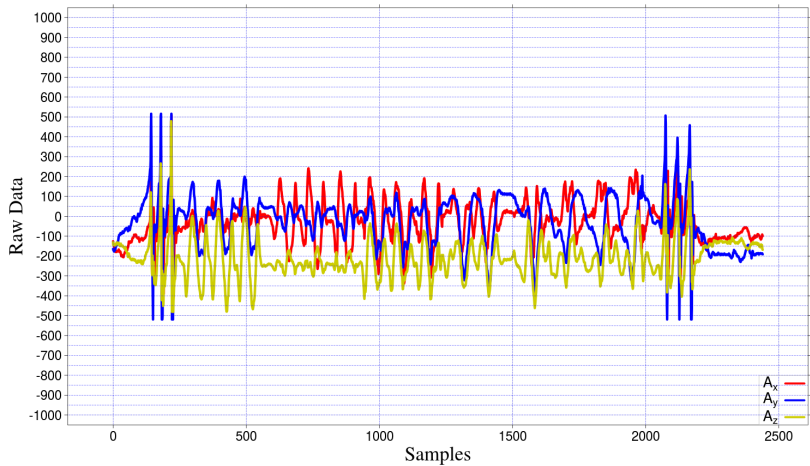


Figure 12: ACC imu0

plotacc imu1 24022016-124306.csv

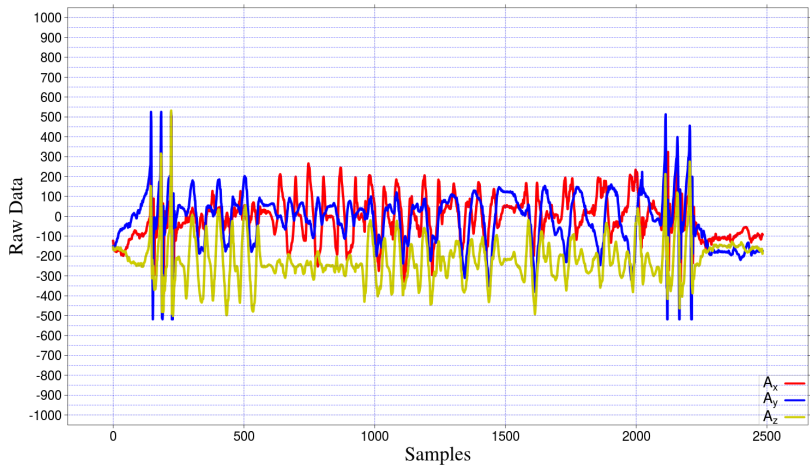


Figure 13: ACC imu1

plotaccRAW Shimmer24022016-1242

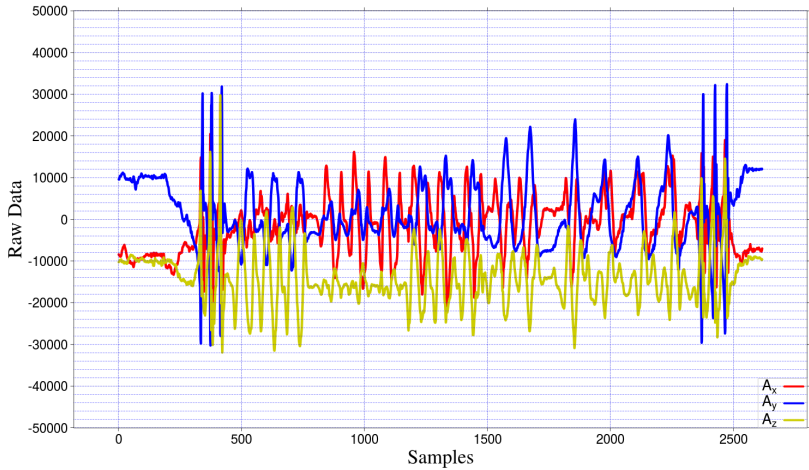


Figure 14: ACC Shimmer

imu0 vs imu1

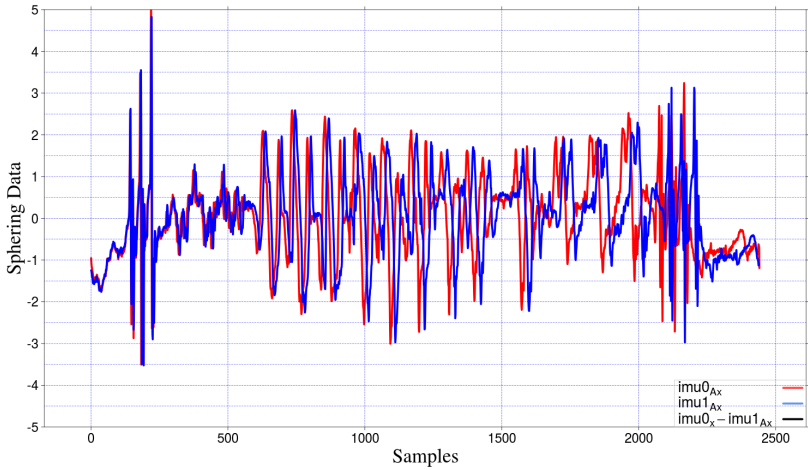


Figure 15: comparison

Shimmer vs imu0

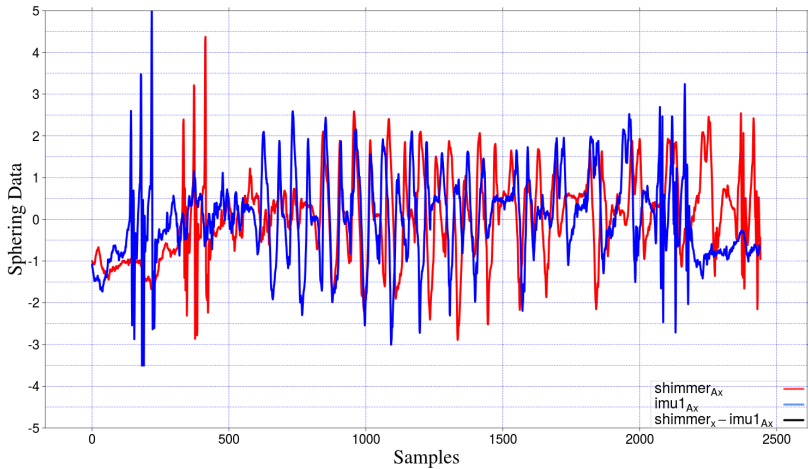


Figure 16: comparison

IMUs Benchmark – Data that other use

Sensor	Price*	Connectivity	ACC	GYR	MAG	Sample rate Hz	Temp.	battery time	API
9 DOF Razor	£59.99	USB,Bluetooth 2.1, LE	Full-scale range: ± 2 g Sensitivity: 256 LSB/g ADCs: 10-bit	Full-scale region: ± 2000 dps Sensitivity: 14.375 LSB/dps ADCs: 16-bit	Full-scale region: ± 8 Gauss Sensitivity: 230 to 1370 LSB/gauss ADCs: 12-bit	50	–	–	C++, Android, ROS
myAHRS+	£69.52	USB,UART,I2C	Full-scale Range: ± 16 g Sensitivity: (2048 LSB/g) ADCs: 16-bit	Full-scale region: ± 2000 dps Sensitivity: 16.4 LSB/dps ADCs: 16-bit	Full-scale Range: ± 1200 T Sensitivity: 0.3 T/LSB ADCs: 13-bit	max 100 Res: 340 LSB/ $^{\circ}$ C	-40 to $+85^{\circ}$ C	–	C++, Python, ROS
EXLs3	€384 ≈ £291	Bluetooth 2.1	Full-scale range: ± 2 / 4/8/16 g	Full-scale range: ± 250 / 500/1000/2000 dps	Full-scale range: ± 1200 dps	5, 10, 12.5, 16.67, 20, 25, 33.33, 50, 100, 200, 300	–	3h	–
WAX9	£178.8	Bluetooth 2.1 and LE	$\pm 2/4/8$ g Resolution: 14-bit	$\pm 250/500/2000$ Resolution: 16-bit	Range ± 1 mT Resolution: 16-bit	1 to 400	0 - 65° C	6h	C#, iOS App
Shimmer3	€503.07** ≈ £381	USB,Bluetooth 2.1	$\pm 2/4/8/16$ g Sensitivity: 1000(2g) /500(4g)/250(8g)/ 83.3(16g) LSB/g ADCs: 16-bit	Range $\pm 250/500/$ 1000/2000 / 131(250) / 65.5 (500) 32.8(1000) / 250 (2000)LBS/g ADCs: 16-bit	Range: $\pm 1.3/1.9/2.5/4.0/$ 4.7/5.6/8.1 Ga Sensitivity: Sensitivity (X,Y,Z) (LSB/Ga): 1100/980(1.3), 855/760(1.9) 670/600(2.5), 450/400(4.0) 400/355(4.7), 330/295(5.6) ADCs: 16-bit 230/205 (8.1) ADCs: (16 bits)	10.24 to 1024	–	14h15m (@51.2Hz)	Matlab LabVIEW C#, Android

*Incl. Tax, ** Incl. shipping *** g is the acceleration due to gravity

PhD Framework for February and March

FEBRUARY

- Create Artificial Structure Signals.
- Apply Statistical and Nonlinear methods to analyse the variability of artificial signals.
- Pilot Data Collection Experiment Using Commercial and non-commercial IMUs.

MARCH

- Pilot classification experiment with SVM or a technique of deep learning
(collaboration with *Dr. Mourad Oussalah*)
- Submit the advances to the International Symposium on Wearable Computers (ISWC) 2016 (Deadline 1st April 16, 2016)

References I

-  Banos, O., Galvez, J.-M., Damas, M., Pomares, H., and Rojas, I. (2014). Window size impact in human activity recognition. *Sensors (Basel, Switzerland)*, 14(4):6474–99.
-  Bulling, A., Blanke, U., and Schiele, B. (2014). A tutorial on human activity recognition using body-worn inertial sensors. *ACM Computing Surveys (CSUR)*, 46(3):1–33.
-  Figo, D., Diniz, P. C., Ferreira, D. R., and Cardoso, J. M. P. (2010). Preprocessing techniques for context recognition from accelerometer data. *Personal and Ubiquitous Computing*, 14(7):645–662.
-  Fish, B. and Khan, a. (2012). Feature selection based on mutual information for human activity recognition. . . . , *Speech and Signal*, pages 1729–1732.
-  Frank, J., Mannor, S., Pineau, J., and Precup, D. (2012). Time Series Analysis Using Geometric Template Matching. *IEEE Transactions on Pattern Analysis and Machine Intelligence*, 35(3):1–1.

References II

-  Frank, J., Mannor, S., and Precup, D. (2010).
Activity and Gait Recognition with Time-Delay Embeddings.
AAAI Conference on Artificial Intelligence, pages 407–408.
-  Gupta, P. and Dallas, T. (2014).
Feature selection and activity recognition system using a single triaxial accelerometer.
IEEE Transactions on Biomedical Engineering, 61(6):1780–1786.
-  Hammerla, N., Ploetz, T., Andras, P., and Olivier, P. (2011).
Assessing Motor Performance with PCA.
Proceedings of the International Workshop on Frontiers in Activity Recognition using Pervasive Sensing (in conjunction with Pervasive 2011), pages 18–23.
-  Liao, M., Guo, Y., Qin, Y., and Wang, Y. (2015).
The application of EMD in activity recognition based on a single triaxial accelerometer.
Bio-Medical Materials and Engineering, 26(s1):S1533–S1539.

References III

-  Plötz, T., Chen, C., Hammerla, N. Y., and Abowd, G. D. (2012).
Automatic synchronization of wearable sensors and video-cameras for ground truth annotation - A practical approach.
Proceedings - International Symposium on Wearable Computers, ISWC, pages 100–103.
-  Samà, A., Ruiz, F. J., Agell, N., Pérez-López, C., Català, A., and Cabestany, J. (2013).
Gait identification by means of box approximation geometry of reconstructed attractors in latent space.
Neurocomputing, 121:79–88.
-  Zhang, M. and Sawchuk, A. A. (2011).
A Feature Selection-Based Framework for Human Activity Recognition Using Wearable Multimodal Sensors.
International Conference on Body Area Networks (BodyNets), 1:92–98.

QUESTIONS?

Miguel Perez-Xochicale

E-Mail: perez.xochicale@gmail.com

Homepage: <https://sites.google.com/site/perezxochicale/>



My own pictures are release under CC BY-NC 4.0

<http://creativecommons.org/licenses/by-nc/4.0/>

Give credits to: Miguel Perez-Xochicale